Anticancer activity of an Artemisia annua L. hydroalcoholic extract on canine osteosarcoma cell lines

Anticancer activity of an Artemisia annua L. hydroalcoholic extract on canine osteosarcoma cell lines

Roberta Salaroli[1], Giulia Andreani[1*], Chiara Bernardini[1], Augusta Zannoni[1], Debora La Mantia[1], Michele Protti[2], Monica Forni[1], Laura Mercolini[2], Gloria Isani[1]

[1]Department of Veterinary Medical Sciences (DIMEVET), Alma Mater Studiorum - University of Bologna, 40064 Ozzano Emilia, Bologna, Italy.

[2] Pharmaco-Toxicological Analysis Laboratory (PTA Lab), Department of Pharmacy and Biotechnology (FaBiT), Alma Mater Studiorum - University of Bologna, 40126 Bologna, Italy*

Corresponding author* at: via Tolara di Sopra 50, 40064 Ozzano Emilia, Bologna, Italy.

E-mail addresses:

roberta.salaroli@unibo.it (R. Salaroli)
*giulia.andreani2@unibo.it (G. Andreani)
chiara.bernardini5@unibo.it (C. Bernardini)
debora.lamantia2@unibo.it (D. La Mantia)
michele.protti2@unibo.it (M. Protti)
monica.forni@unibo.it (M. Forni)
laura.mercolini@unibo.it (L. Mercolini)
gloria.isani@unibo.it (G. Isani)

Abstract

Since ancient times, *Artemisia annua* (*A. annua*) has been used as a medicinal plant in Traditional Chinese Medicine. In addition, recent studies have investigated the cytotoxic effects of *A. annua* extracts towards cancer cells. The leading aim of the present research is to evaluate the cytotoxic effects of an hydro alcoholic extract of *A. annua* on two canine osteosarcoma (OSA) cell lines, OSCA-8 and OSCA-40, focusing on the possible involvement of ferroptosis.

The quantitative determination of Artemisinin concentration in the extract, culture medium and OSA cells was carried out through the use of an instrumental analytical method based on liquid chromatography coupled with spectrophotometric detection and tandem mass spectrometry (HPLC-DAD-MS/MS). OSCA-8 and OSCA-40 were exposed to different dilutions of the extract for the EC_{50} calculation then the uptake of Artemisinin by the cells, the effects on the cell cycle, the intracellular iron level, the cellular morphology and the lipid oxidation state were evaluated. A concentration of Artemisinin of 63.8 ± 3.4 µg/mL was detected in the extract. A dose-dependent cytotoxic effect was evidenced. In

OSCA-40 alterations of the cell cycle and a significantly higher intracellular iron content were observed. In both cell lines the treatment with the extract was associated with lipid peroxidation and with the appearance of a “ballooning” phenotype suggesting the activation of ferroptosis. In conclusion the *A. annua* idroalcoholic extract utilized in this study showed anticancer activity on canine OSA cell lines that could be useful in treating drug resistant canine OSAs.

Keywords: *Artemisia annua*, canine osteosarcoma cell lines, iron, lipid peroxidation, balloning phenotype, ferroptosis.

1. Introduction

Extracts of *Artemisia annua* L. are well-known remedies in Chinese Traditional Medicine and have been used to treat malaria and fever in Asia and Africa [1]. *A. annua* is characterized by the unique presence of artemisinin, a sesquiterpene trioxane lactone, which contains an endoperoxide bridge essential for its bioactivity. Artemisinin and its derivatives demonstrated also anticancer activity in

different human and animal cancer cell lines [2], targeting different pathways, including inhibition of cell proliferation, induction of apoptosis, and inhibition of angiogenesis and metastasis [3]. In addition, artemisinin reveals an additional anticancer mechanism through induction of ferroptotic cell death [4]. To sustain increased proliferation, tumour cells have high iron requirement, a phenomenon also known as “iron addiction” and are characterized by high intracellular iron content [5]. The endoperoxide bridge of artemisinin is strategic for its pharmacological activity, in fact its cleavage leads to the formation of radical species and induces oxidative stress [6]. In addition, in the presence of reduced ferrous ions or heme iron, artemisinin can become a potent alkylating agent, capable of inducing direct oxidative damage. Consequently, an iron-mediated lethal lipid peroxidation called ferroptosis can occurs in cancer cells leading to cell death [7, 8]. Thus, iron plays an important role in the selective toxicity of artemisinin towards cancer cells.

Osteosarcoma (OSA) is the most common primary bone tumour in dogs and humans [9-11]. In veterinary medicine, OSA accounts for 2-5% of all canine neoplasms [7] and 80-85% of all bone tumours [12].

A study on 162 dogs with appendicular osteosarcoma reported a median survival of 19.2 weeks. The one-year and two-year survival rates are 11.5% and 2%, respectively. Many dogs die or are suppressed due to the presence of pulmonary metastases [13]. Current treatment for canine OSA (cOSA) involves surgery to remove primary tumours; however, dogs treated with surgery alone have a short survival time. Surgery combined with chemotherapy can increase the survival of dogs with OSA, and protocols include doxorubicin, cisplatin, and carboplatin used alone or in combination [12]. However, drug resistance is a critical issue determining the failure of therapy in many cases. Therefore, it would be of paramount importance implement the choice of possible drugs to be used in chemotherapy and also to provide low-cost treatment for those animals that do not have access to chemotherapy for economic reasons. Two previous *in vitro* studies have demonstrated the cytotoxicity of dihydroartemisinin on different cOSA cell lines [14] and of an hydroalcoholic extract and pure artemisinin on cOSA D-17 cell line [15, 16].

The aim of this research is to deepen the knowledge on the cytotoxic and anti-proliferative effects of an

hydroalcoholic commercial extract of *A. annua* on two additional canine osteosarcoma cell lines, OSCA-8 and OSCA-40, focusing on the possible involvement of ferroptosis. In detail, to provide more specific therapeutical indications, the aims of the work were to determine: i) the concentration of Artemisinin in the phytoextract and in the culture media and cells after the treatment; ii) the cytotoxicity and the anti-proliferative effects of the extract; iii) the intracellular iron content alteration following the treatment. All tests have been performed for comparison also with the primary compound Artemisinin.

2. Materials and Methods

Cells, chemicals and reagents

Canine osteosarcoma cell lines OSCA-8 and OSCA-40 were purchased from Kerafast, Inc. (Boston, MA, USA). Minimum Essential Medium (MEM) with GlutaMAX, Foetal Bovine Serum (FBS), Antibiotic-Antimycotic solution, Dulbecco Phosphate Buffered Saline (DPBS), DPBS without calcium and magnesium (PBS w/o Ca^{2+} and Mg^{2+}), RNaseA/T1 were purchased from Thermo Fisher Scientific

(Waltham, MA, USA). Dimethyl Sulfoxide (DMSO), Fluoroshield™ histology mounting medium and erastin were purchased from Merck (Darmstadt, Germany). Propidium iodide (PI) and Hoechst 33342 staining solution were purchased from Miltenyi Biotec (Bergisch Gladbach, Germany). Lipid Peroxidation Assay Kit was purchased from Abcam (Cambridge, UK). All plastic supports for cell culture and 8-well slide chambers were purchased from Corning-Beckton-Dickinson (Franklin Lakes, NJ, USA). Artemisinin (CAS number: 63968-64-9), acetonitrile, methanol, formic acid (all mass spectrometry-grade) were obtained from Sigma Aldrich (St. Louis, MO, USA). Artemisinin-D3 pure powder, used as the internal standard (IS), was provided by Biosynth (St. Gallen, Switzerland). All solutions used for LC-DAD-MS/MS analysis were stored protected from light in amber glass vials certified for mass spectrometry from Waters Corporation (Milford, MA, USA). A commercial hydroalcoholic extract obtained from aerial parts of *A. annua* and composed by 65% ethanol, 20% of aerial parts and water was used (*Artemisia annua* hydroalcoholic solution, Sarandrea Marco C. srl, Fr, Italy).

MEPS-LC-DAD-MS/MS determination of artemisinin

Quali-quantitative analytical determinations were carried out exploiting a previously developed and fully validated methodology based on microextraction by packed sorbent (MEPS) coupled to liquid chromatography with diode array detection and tandem mass spectrometry (LC-DAD-MS/MS) for the determination of Artemisinin in extracts and commercial products [17]. Briefly, LC-DAD-MS/MS analysis was performed using a Waters (Milford, MA, USA) Alliance e2695 chromatographic system equipped with autosampler coupled to a Waters 2998 photodiode array detector and a Waters Micromass Quattro Micro triple-quadrupole mass spectrometer, interfaced with an electrospray ion source working in positive ionisation mode (ESI+). Chromatography was obtained a Restek (Bellefonte, PA, US) Ultra AQ reverse-phase C18 column (50 × 2.1mm I.D., 3µm), kept at room temperature and equipped with a C18 guard column (10 × 2.1mm I.D., 3µm), while injection volume was 10 µL. An automated composition gradient program managed a 2-component mobile phase composed of 0.25% formic acid in water (component A) and 0.25% formic acid in acetonitrile

(component B), flowing at a constant rate of 0.2 mL/min: T=0 min, A:B 70:30; T=2 min, A:B 10:90; T=5 min, A:B 10:90; T=6 min, A:B 70:30; T=8, A:B 70:30. To detect Artemisinin, DAD was set at 232 nm, while for MS/MS analysis, multiple reaction monitoring (MRM) was used exploiting two different exclusive *m/z* transitions (one for quantitative purposes, one for qualitative confirmation) for both Artemisinin (283.24 → 209.45; 283.24 → 265.36) and Artemisinin-D3, used as internal standard (IS, 286.31 → 212.38; 286.31 → 268.34). For sample pretreatment, all the samples involved in this study (hydroalcoholic extract, cell pellets and cell culture supernatant) were subjected to MEPS pretreatment before LC analysis. Cell pellets from $1x10^6$ cells were preliminarily homogenized in 0.1 M, pH 5.5 sodium phosphate buffer (1 mL/sample). The mixtures were centrifuged at 4000 rpm for 10 min (4 ◦C) and the supernatants were collected. 100-µL aliquots of the hydroalcoholic extract/cell pellet extract/cell culture supernatant were then subjected to a MEPS following a protocol developed ad-hoc for Artemisinin analysis and involving a miniaturised apparatus based on C8 sorbent [17].

Cell culture and treatments

OSCA-8 and OSCA-40 were cultured in MEM with GlutaMAX, 5% foetal bovine serum (FBS) and 1% antibiotic/antimycotic solution and expanded in T-25 or T-75 culture flasks at 2.5 x 10^4 cells/cm^2 seeding density, at 37°C and 5% CO_2. The commercial extract was directly diluted in the culture medium to obtain the required artemisinin concentrations, based on the artemisinin concentration determined in the phytoextract as previously described. Artemisinin powder was firstly dissolved in DMSO and then diluited in the culture medium. Control cells were treated with equivalent amount of ethanol (ranging dilution 0.3-10%) or DMSO (0.05-3%) used as specific vehicles.

Cytotoxicity and EC_{50} determination

The two cell lines were seeded in 96-well plates (1x10^4 cells/well) and exposed, for 24 h, to increasing doses of *A. annua* hydroalcoholic extract corresponding to Artemisinin concentrations of 0, 0.22, 0.44, 1.1, 2.2, 4.4, and 35.2 µM, calculated on the measured concentration of Artemisinin in the hydroalcoholic extract or with increasing concentrations of pure Artemisinin (0, 50, 100, 500, 1000, 2000, 3000 µM). Cytotoxicity was measured

using tetrazolium salt (In Vitro Toxicology Assay Kit, MTT-based). Briefly, the MTT substrate was added to the culture medium and incubated for 3 h, then the MTT solubilization solution was added to the cells to dissolve the formazan crystals. The formazan absorbance was measured at a wavelength of 570 nm, using Infinite® F50/Robotic Absorbance microplate readers (TECAN, LifeScience). The background absorbance of multiwell plates at 690 nm was also measured and subtracted from the 570 nm measurements. EC_{50} values were calculated from dose-response curves using nonlinear regression analysis tool in GraphPad Prism 7 software [log(agonist) vs. normalized response - Variable slope] (GraphPad San Diego, CA, USA). Each assay was performed thrice independently, with seven replicates each.

Cell cycle analysis

OSCA-8 and OSCA-40 cells were seeded ($2.5x10^5$) in 6-wells plates in complete medium and, when confluence reached round about 70%, cells were treated with *A. annua* hydroalcoholic extract and with Artemisinin EC_{50} doses for 24 h in a humidified CO_2 incubator. EtOH and DMSO exposed cells were

considered as controls as described above. After 24 h of treatment, cells were harvested, counted, washed twice in 5 mL of DPBS w/o Ca^{2+} and Mg^{2+} then fixed overnight in 70% ice-cold EtOH (1mL/1x10^6 cells) added drop-by-drop under continuous vortex mixing. After fixation, the cells were washed with 10 mL DPBS w/o Ca^{2+} and Mg^{2+} and cellular pellet was incubated with 1mL/10^6 cells of staining solution [50 µg/mL PI + 100 µg/mL RNaseA/T1 in DPBS w/o Ca^{2+} and Mg^{2+}] for 30 min in the dark at room temperature (RT). The DNA contents 2N (G0/G1 phase), 2– 4N (S phase), and 4N (G2/M phase) were evaluated by MACSQuant® Analyzer10 (Miltenyi Biotec, Bergisch Gladbach, Germany) and Flow Logic software (Inivai Technologies, Australia) as previously described [18]. Dean-Jett-Fox Univariate Model was used to determine the percentage of the cell population in the distinct phases of the cell cycle [19]. The experiment was repeated three times.

Iron quantification in OSCA-8 and OSCA-40

For the quantification of intracellular iron, cells were seeded and grown in wells as previously described. Then, cells were treated with *A. annua* hydroalcoholic

extract or Artemisinin at the respective EC_{50} doses, for 24 h. After the treatment cells were harvested and centrifuged at 800 x g for 10 min. The pellet was washed twice with DPBS, and then $1x10^6$ cells were resuspended in 1 ml of a solution of 1 M HNO_3, digested at room temperature until completely dissolved, and finally used for iron quantification using a Spectra AA-20 atomic absorption spectrometer (Varian) equipped with a GTA-96 graphite tube atomizer and a sample dispenser. Final data were expressed as pg Fe/cell.

The optimization of the analytical method was obtained following Tüzen [20] with minor changes. The graphite tubes employed were coated GTA tubes (Agilent Technologies, Germany), the hollow cathode lamp current was 7 mA and measurements were performed at 248.3 nm resonance lines using a spectral slit width of 0.2 nm. During spectrophotometer readings, internal argon flow rate in the partition graphite tubes was maintained at 300 mL/min and was interrupted in the atomization phase. Ramp and hold times for drying, pyrolysis, atomization and cleaning temperatures were optimized to obtain maximum absorbance without

significant background absorption, therefore, background correction was not necessary.

The calibration curve was obtained by diluting 1 mg/mL standard stock solution of iron (Iron Standard for AAS, Sigma-Aldrich, St Louis, Missouri, USA) with Suprapur water (Supelco, St Louis, Missouri, USA) to obtain working standards containing 0, 20, 40 and 60 ng/mL of iron and by plotting the absorbance at 248.3 nm against iron concentrations. The equation of the curve was y = 0.0121x and the calculated regression coefficient (r) was 0.996. The method was validated with standard reference material (ERM® - BB422) and the accuracy of the method, calculated as the percentage of the certified value, resulted of 106 %. The detection limit (LOD), defined as the concentration corresponding to 3 times the standard deviation of 6 blanks, was 0.8 ng/mL

Light microscopic evaluation

OSCA-8 and OSCA-40 cell lines were treated for 24 h with *A. annua* hydroalcoholic extract, Artemisinin at the EC_{50} dose or with erastin (10 µM) that triggers ferroptosis [21], an iron-dependent form of non-apoptotic cell death. The cell death morphology was observed and acquired using an inverted microscope

(Eclipse TS100, Nikon, Tokyo, Japan) equipped with a digital camera (Digital C-Mount Camera TP3100, Kowa, Aichi, Japan).

Lipid Peroxidation Assay

Lipid peroxidation in OSCA-8 and OSCA-40 treated with *A. annua* hydroalcoholic extract or with Artemisinin was evaluated by the Lipid Peroxidation Assay Kit (Abcam, Cambridge, UK) following manufacturer's instructions. The day before the experiment $1x10^5$ cells/well were seeded in 8 well chamber slides and the cells were incubated for 24 h with *A. annua* hydroalcoholic extract, with Artemisinin at the respective EC_{50} doses or with vehicle controls. To have positive controls OSCA-8 and OSCA-40 were treated with erastin (10 µM) for 24 h. Lipid Peroxidation Assay Kit uses a sensitive sensor that changes its fluorescence from red to green upon peroxidation by ROS in cells. The cells were also stained with Hoechst 33342 during the last 10 minutes of incubation with lipid peroxidation sensor. Fluorescence of the cells was monitored with a fluorescence microscope (Eclipse E600, Nikon) equipped with a digital camera (RETIGA-2000RV, Surrey, Canada) through FITC/TRITC channels.

Statistical analysis

Data for MTT were analysed with one-way analysis of variance (ANOVA) followed by post hoc Dunnett's multiple comparison test. Data of the cell cycle and iron content were analysed by paired Student's t-test. $p < 0.05$ was considered significant.

3. Results and discussion

Quantification of artemisinin in *A. annua* extract and artemisinin cOSA uptake

For this purpose, a very sensitive method was developed, based on high performance liquid chromatography coupled to diode array detection and tandem mass spectrometry (HPLC-DAD-MS/MS). This method was previously validated with satisfactory results in terms of sensitivity (LOQ=5 ng/mL and LOD=1.5 ng/mL), linearity (r^2 > 0.9995 over the 5-1000 ng/mL artemisinin concentration range), extraction yield (>85 %), precision (RSD%<3.5) and accuracy (88-93% range), allowing an accurate determination of artemisinin concentrations in different matrices.

In the hydroalcoholic extract of *A. annua* considered in this study, a concentration of artemisinin of 63.8 ±

3.4 µg/mL, corresponding to 0.23 mM, was detected. The value is in accordance with those reported by Protti et al. (2019) [17]. In that research, extracts prepared ad hoc from herbal material by the authors were analysed (Artemisinin concentration was 21.40 µg/mL for the hydroalcoholic extract and 109.40 µg/mL for the artemisinin-enriched extract prepared following Chinese Pharmacopeia), as well as a commercial extract sold as food supplement (94.79 µg/mL). The results obtained in this study are also consistent with previously reported data, even if Artemisinin concentration shows a pronounced variability depending on the source, ranging from 60 µg/mL [22] to 200-500 µg/mL [23].

To verify the uptake of artemisinin by the cells, Artemisinin content was determined either in the incubation media or in the OSCA-8 and OSCA-40 cell lines after 24 hours of exposure to *A. annua* extract or Artemisinin at the EC_{50} doses (Table 1). Cells actively took up Artemisinin, which reached a concentration of 1.66 pg/cell in OSCA-40 cell line. In both cell lines, the intracellular concentration of Artemisinin is higher in the case of exposure to pure Artemisinin than to the phytoextract, in agreement

with the higher concentrations in the medium and higher EC_{50} values.

The innovative analytical method gave the opportunity to accurately determine the concentration of Artemisinin taken up by cells and allowed an evidence-based discussion of the cytotoxic effects of the extracts.

Table 1. Artemisinin concentration determined in culture medium and in OSCA-8 and OSCA-40 cell lines after 24 hours of exposure to pure Artemisinin (A) and *A. annua* extract (E) at the EC_{50} doses.

	Medium µg/mL	Intacellular Artemisinin pg/cell
OSCA-8 (A)	4.05	2.54
OSCA-8 (E)	0.41	1.36
OSCA-40 (A)	3.76	2.42
OSCA-40 (E)	0.38	1.66

Artemisia annua hydroalcoholic extract is cytotoxic for canine OSA cell lines

MTT assay was used to determine the effect of an *A. annua* hydroalcoholic extract containing 63.8 µg artemisinin/mL or primary compound Artemisinin on the growth of 2 different canine OS cell lines: OSCA-8 e OSCA-40. The *A. annua* hydroalcoholic extract showed a dose-dependent cytotoxic effect inhibiting the proliferation of the two canine OSA cell lines with EC_{50} of 3.3 and 2.6 µM for OSCA-8 and OSCA-40 respectively, while Artemisinin showed an EC_{50} of 2548 µM for OSCA-8 and of 878.3 µM for OSCA-40. (Figure 1). Accordingly, a similar toxic effect was previously reported for D-17 canine OSA cell line by Isani et al., (2019) [15] and a marked dose-dependent toxic effect of an extract of *A. annua,* obtained by pressurized cyclic solid–liquid extraction, was reported by Culurciello et al. (2021) [16] on a different canine OS cell line (CRL2130). The extract presented significantly lower EC_{50} values than Artemisinin (Fig. 1). The EC_{50} values for Artemisinin determined in this study are one-order magnitude

lower than those reported for pure Artemisinin in two other canine tumour cell lines, DH82 and D-GBM, by Saeed et al. (2020) [24], suggesting a more potent cytotoxic effect of the phytoextract. Indeed, the extract contains many other cytotoxic compounds in addition to Artemisinin, including polyphenols, flavonoids, coumarins, and phytosterols. Important constituents are camphene, camphor, beta-caryophyllene, pinene, 1,8-cineole, and scopoletin [25]. Volatile essential oils are also present at concentrations of 0.20-0.25%. All these secondary metabolites acting in a multi-specific manner against tumours can contribute to the toxic effect of the phytoextract [26]. The data reported in the present research add more evidence on the potency of *A. annua* extracts, which inhibit the growth of canine osteosarcoma cells, and might be considered promising anti-tumour candidate for further development.

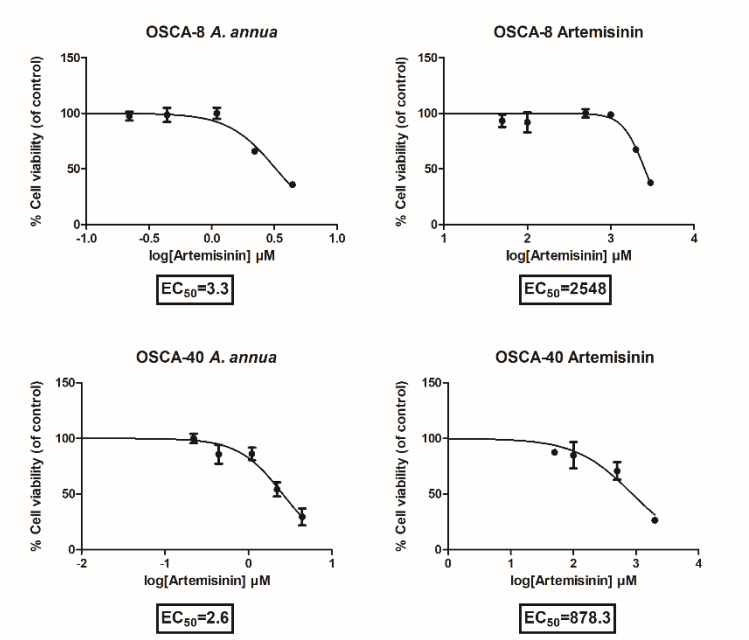

Figure 1_ *A. annua* hydroalcoholic extract and Artemisinin impair cell viability of the canine OSA cell lines OSCA-8 and OSCA-40. The cells were treated with increasing concentrations of *A. annua* hydroalcoholic extract, Artemisinin or vehicles for 24 h and the cell viability measured by MTT assay. Dose-response curves represent mean ± SD from three independent experiments with seven replicates each(n=3).

The cytotoxic effects of *A. annua* could be related to DNA damage, oxidative stress, and alteration of tumour-related signal transduction pathways [2, 24]. The effect of the extract on cell cycle was evaluated by flow cytometry and data were analysed with Flow Logic software. The cells grew as asynchronous populations represented by cells in all stages of the cell cycle. For OSCA40 cell line treated with *A. annua* extract and with Artemisinin at the EC_{50} doses, the

gates were inserted manually because Dean-Jett-Fox Model failed to distinguish the different phases of the cell cycle. Considering the cells treated with the vehicles (EtOH or DMSO) as control, it can be observed that *A. annua* extract and Artemisinin treatments impair the cellular distribution in the different cell cycle phases. Particularly, in OSCA-8 cell line pure Artemisinin, but not *A. annua* extract, determined a significant decrease ($P<0.05$) of the cells in G0/G1 accompanied by a significant increase ($P<0.001$) of the cells in sub-G0/G1 phase. In OSCA-40, both treatments strongly influenced the cell distribution with significant decrease ($p<0.05$) of the cells in G0/G1 accompanied by a significant increase ($p<0.001$) of the cells in sub G0/G1 phase. (Fig. 2,3). These data add further evidence to the effects of Artemisinin on the cell cycle.

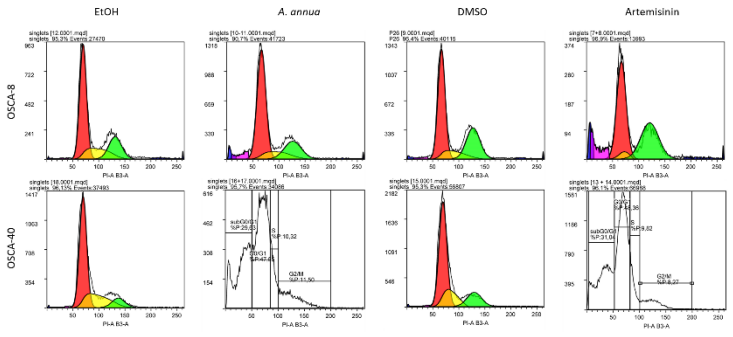

Figure 2_ *A. annua* hydroalcoholic extract and Artemisinin impair cell cycle of the canine OSA cell lines. The cells were treated with *A. annua* extract and Artemisinin at the EC_{50} doses

505 or vehicle (EtOH or DMSO) for 24 h and fluorescence of the PI-
506 stained cells was measured using MACSQuant® Analyzer10
507 and analysed by Flow Logic software (Inivai Technologies,
508 Australia). 5 × 10^5 cells were examined for each sample and
509 experiment was repeated three times. Representative DNA
510 content frequency histograms in OSCA-8 and OSCA-40. Sub
511 G0/G1 blue/purple, G0/G1 red, S yellow, G2/M green.

512

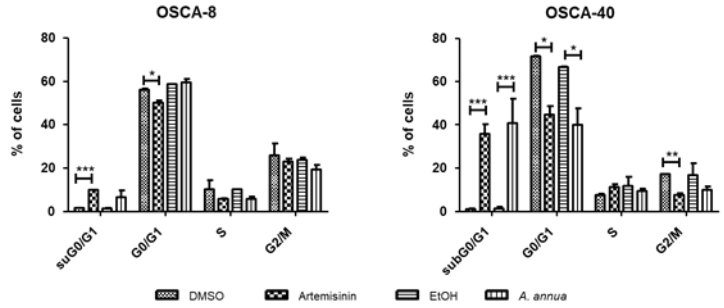

513

514 **Figure 3_ Grouped histograms graphs of cell cycle**
515 **distribution in OSCA-8 and OSCA-40.** The cell lines were
516 treated with *A. annua* hydroalcoholic extract and Artemisinin at
517 the EC_{50} doses for 24 h or vehicles (EtOH or DMSO). Cell
518 percentages were averaged over triplicate samples, and the
519 data are expressed as the mean ± SD. Paired Student's t-test,
520 (*p<0.05, **p<0.01; ***p<0.001) was performed between
521 controls and treated cells (n=3).

522 As a matter of fact, Artemisinin and its derivatives
523 (dihydroartemisinin, artesunate, artemether,
524 arteether) are known to affect the cell cycle of several
525 types of tumour cells in different ways, depending on
526 specific defects of the machinery regulating the cell

cycle of tumour cell lines [27]. In OSCA-8 the exposure to pure Artemisinin but, in OSCA-40, also the exposure to *A. annua* extract induced a significant decrease of the cells in G0/G1 accompanied by a significant increase of the cells in sub G0/G1 phase. The same profile was also reported for other canine and human OSA cell lines treated with dihydroartemisinin [14, 28]. A dose-dependent accumulation of MDA-MB-468 and SK-BR-3 breast cancer cells in the sub-G1 fraction following the exposure to artesunate, a semi-synthetic derivative of Artemisinin, has been reported also by Greenshields et al. (2019) [29]. Sub-G0/G1 peak is composed by dead cells (apoptosis, necrosis, oncosis) and by cells that had already lost their DNA by shedding apoptotic bodies, cellular fragments holding pieces of chromatin, broken nuclei, chromosomes, and cellular debris [30]. It could be hypothesised that Artemisinin in *A. annua* hydroalcoholic extract extensively impairs DNA integrity in OSCA-40 cells and an efficient G1 checkpoint machinery hosted by this canine OSA cell line leads cells to die before replicating their damaged DNA. The DNA damage response (DDR) is a complex system, a network of biochemical

552 pathways that detects DNA damage and decides the
553 cell fate. These pathways include the repair
554 throughout different phases of proliferation, the delay
555 of cell cycle, and the arrest of cell cycle to allow for
556 more comprehensive DNA repair [31]. If the level of
557 DNA damage exceeds the cells repairing ability, cell
558 death is stimulated. DNA damage is caused by
559 various internal and extrinsic factors including
560 reactive oxygen species (ROS) and environmental
561 mutagens [32]. In OSCA-8 cell line, where only pure
562 Artemisinin is able to impair the cell cycle, the DNA
563 damage induced by *A. annua* might be less extensive
564 and unable to lead to a significant cell cycle
565 impairment or the cellular repair machinery could be
566 so efficient to allow a complete repair. This
567 hypothesis is supported by the lower intracellular
568 concentration of Artemisinin measured in OSCA-8
569 (Table 1).

570 ***Artemisia annua* hydroalcoholic extract modifies**
571 **intracellular iron content in canine OSA cell line**

572 Tumours are characterized by high iron content, to
573 satisfy their increased metabolic demand [5]. This is
574 achieved through some crucial changes in iron
575 metabolism, including the increased expression of

transferrin receptor-1 (TfR1) in many tumours [33], including cOSA [34]. The intracellular iron content influences the sensitivity of cells to ferroptosis. As a result, to study the iron involvement in the cytotoxicity of *A. annua* extract the need arose to measure the iron content in OSCA-8 and OSCA-40 cell lines with a sensitive and accurate method. This is a challenging task, due to the very small amount of the biological samples; consequently, a specific elemental detector with low detection limit is needed. Complex analytical methods with different degree of accuracy and sensitivity are currently available to measure iron in cells, including FAAS, ICP-MS and TXRF [35]. The analytical FAAS method used in this research with a detection limit of 0.8 ng/mL was able to detect iron in all the samples analysed. Iron content in cells is reported in Figure 4. The variety of analytical methods and the related different units of measurement to express the intracellular iron content hamper the comparison with the data in the literature. Iron content in control untreated cells is like the value reported in canine D-17 OSA cells [15], if expressed as ng/1x10^6 cells. OSCA-40 cells treated with *A. annua* extract at the EC_{50} dose had a significantly ($p<0.05$) higher iron content than those treated with

601 the vehicle, while no significant difference was
602 detected for OSCA-8. An increase of intracellular iron
603 content, though measured with a less accurate and
604 specific colorimetric method, was also reported in
605 Saos-2 and U2os human OSA cell lines treated with
606 EF24, a synthetic analogue of curcumin [36]. In both
607 cell lines, no significant effect of Artemisinin was
608 detected in comparison with the vehicle (Figure 4).

609

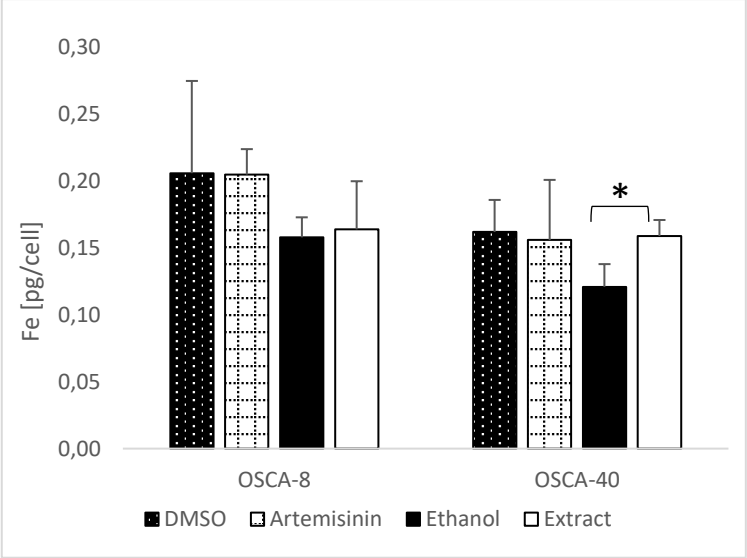

610

611 **Figure 4_ Intracellular iron content in OSCA-8 and OSCA-**
612 **40.** The vehicles (DMSO for Artemisinin and 65% EtOH for
613 extract) were used as control. Data are expressed as pg Fe/cell
614 and are reported as mean ± SD from three independent
615 experiments (n=3), each performed in duplicate. Paired
616 Student's t-test, (*$p<0.05$) was performed between control and
617 treated cells.

Artemisia annua hydroalcoholic extract induces "ballooning" phenotype in canine OSA cell lines

Cells were exposed for 24 h to *A. annua* hydroalcoholic extract or to Artemisinin at the EC_{50} doses and to 10 μM erastin to investigate the possible involvement of ferroptosis. Erastin, a well-known inducer of ferroptosis, inhibits cystine uptake by the cystine/glutamate antiporter (system xc −), decreasing the antioxidant defences of the cell, and ultimately leading to oxidative cell death [21]. Ferroptosis is dependent upon intracellular iron and is morphologically, biochemically, and genetically distinct from apoptosis, necrosis, and autophagy [21]. It is known that, following the treatment with a pro-ferroptotic agent such as erastin, an initial cell shrinking is followed by condensation of cytoplasmic constituents and a "ballooning" phenotype, which involves the formation of a clear, rounded morphology consisting mainly of empty cytosol. The exact mechanisms underlying the phenotypic changes that occur during ferroptosis remain unclear [37]. In both cell lines treated with *A. annua* hydroalcoholic extract or with 10 μM erastin, and in OSCA-40 cells treated with pure Artemisinin, the microscopic examination revealed loss of attachment

to the culture plate and dead cells showed a clear "ballooning" phenotype suggesting that not only erastin but also *A. annua* could trigger ferroptosis in canine OS cell lines. (Fig. 5 b, c, f, g and h) In contrast, the cells treated with the vehicle (EtOH) had no evidence of cytotoxicity nor of such specific phenotype. (Fig. 5 a, e). On the other hand, the OSCA-8 cells treated with pure Artemisinin showed evidence of cytotoxicity, but not a clear "ballooning" phenotype. (Fig. 5d)

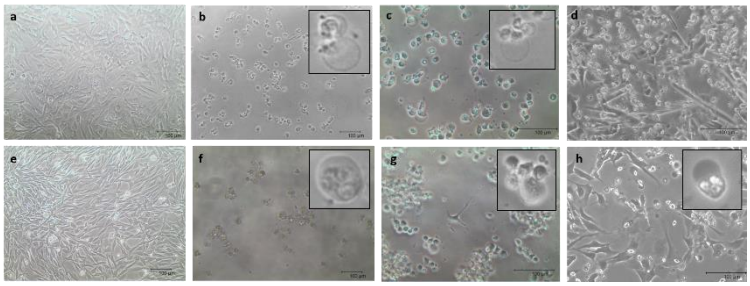

Figure 5_ *A. annua* hydroalcoholic extract induces "ballooning" phenotype in canine OSA cell lines OSCA-8 and OSCA-40. Representative images of OSCA-8 (a, b, c, d) and OSCA-40 (e, f, g, h) treated with *A. annua* hydroalcoholic extract at the EC_{50} dose (b, f), erastin 10µM (c, g) or EtOH (a, e). Following the treatment with *A. annua* hydroalcoholic extract or erastin 10µM bothcell lines showed a "ballooning" phenotype which involves the formation of a clear, rounded morphology consisting mainly of empty cytosol (see in the boxes). In OSCA-

40, pure Artemisinin treatment induced a “ballooning” phenotype. Scale bar: 100 µm.

Artemisia annua hydroalcoholic extract induces Lipid Peroxidation in canine OSA cell lines

In OSCA-8 and OSCA-40 canine OSA cell lines, the treatment with *A. annua* hydroalcoholic extract and with pure Artemisinin at the EC_{50} doses for 24 h leads to extensive lipid peroxidation as indicated by a clear shift from red to green of the Lipid Peroxidation Sensor (Fig. 6). Lipid peroxidation is an oxidative degradation and ROS play a dual role, beneficial and/or deleterious. Indeed, a growing body of evidence shows that within cells ROS act as secondary messengers in intracellular signalling cascades, inducing and maintaining the oncogenic phenotype of cancer cells both in humans and dogs [38, 39]. However, ROS can also induce cellular senescence, apoptosis, ferroptosis and can therefore function as anti-tumourigenic species [38]. Artemisinin and its derivatives induce ROS overproduction, triggering peroxidation of membrane lipids and cell death in a wide range of cellular types, including plants, and mammalian cancer cells [8, 40]. The increase of ROS production in a dose-dependent

manner was also reported by Hosoya et al. (2008) [14] in D-17 cOSA cell line treated with dihydroartemisinin. Since ferroptosis is associated with accumulation of lipid peroxides [21, 37] it could be further speculated that the cytotoxicity of *A. annua* involves ferroptotic cell death.

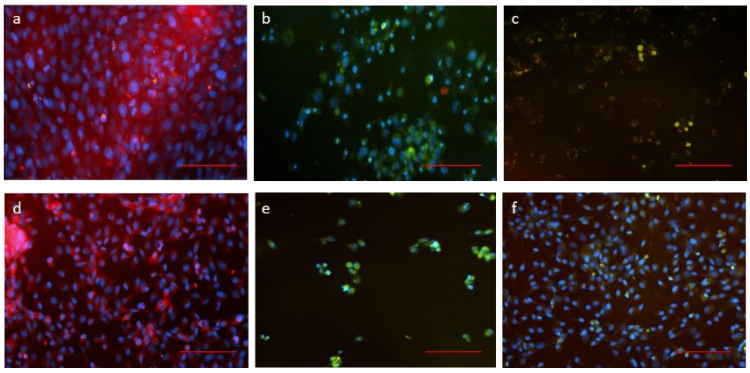

Figure 6_*A. annua* hydroalcoholic extract induces Lipid Peroxidation in canine OSA cell lines OSCA-8 and OSCA-40. Representative images of OSC-8 (a, b, c) and OSCA-40 (d,e,f) treated with *A. annua* hydroalcoholic extract at the EC_{50} dose (b, e), with pure Artemisinin at the EC_{50} dose (c,f) and controls (untreated cells, a, d). The cells were stained with 1X Lipid Peroxidation Sensor for 30 minutes in complete growth medium at 37°C and stained with Hoechst 33342 during the last 10 minutes of incubation. In b, c, e and f a clear shift from red to green was observed. Scale bar: 100 µm.

Involvement of ferroptosis

711 Three main traits define ferroptotic cell death, namely
712 the increase of free iron, the accumulation of lipid
713 peroxides, and a “ballooning” death phenotype that is
714 morphologically distinct from autophagic, apoptotic,
715 or necrotic cell death phenotypes [21]. In both cell
716 lines, *A. annua* hydroalcoholic extract at the EC_{50}
717 doses triggered the appearance of a “ballooning”
718 phenotype as well as extensive lipid peroxidation,
719 while the iron content increased in OSCA-40, but not
720 in OSCA-8. Alteration of iron metabolism is
721 recognized as central mediator of ferroptosis. Ferric
722 ions bound to transferrin are imported into cells using
723 the transferrin receptor 1 (TFR1) and then included in
724 the endosome. In the endosome, ferric ions are
725 reduced to ferrous ions and finally transported into
726 the cytoplasm through the divalent metal transporter
727 1 (DMT1). In the cell cytoplasm a dynamic and
728 controlled labile iron pool (LIP) is present and serves
729 as a crossroad of intracellular iron metabolism [41].
730 In normal cells, this pool is maintained within a
731 narrow range of concentration, while in cancer cells,
732 a reduction of ferritin iron storage can increase the
733 LIP and the risk of oxidative stress, which in turn is
734 able to determine a massive lipid peroxidation. In
735 different human tumour cell lines, including OSA,

exposed to dihydroartemisinin an increase of LIP has been reported, due to the increased lysosome-mediated ferritin degradation [8]. However, despite an increasing number of studies, the role of iron in ferroptotic cell death is still to be completely understood, due to the complexity of iron metabolism and homeostasis. OSCA-40 cell line is more sensitive to the cytotoxic effect of the extract, has a lower EC_{50} value for *A. annua* extract and or pure Artemisinin, a higher intracellular Artemisinin and iron content, and extensive lipid peroxidation associated with a “ballooning” phenotype appeared following the exposure to *A. annua* extract and to pure Artemisinin for 24 hours. This experimental evidence argues in favour of the activation of ferroptosis. Although the method for iron analysis used in this research allows the quantification of total intracellular iron, an imbalance of its metabolism can be hypothesised, leading to an increased ferritin degradation and finally to increased LIP. In OSCA-8 treated with *A. annua* extract, even in the presence of the “ballooning” phenotype and lipid peroxidation, no increase in total iron content and no impairment of cell cycle were observed. However, it cannot be excluded an increase of LIP without modifying the

761 intracellular content of iron as well as a different
762 kinetics in DNA damage response mechanisms in the
763 two cell lines.

764 The high chemoresistance is a negative trait of most
765 OS [42] and ferroptosis is considered as an
766 interesting therapeutic strategy to overcome
767 multidrug resistance. Recently, it has been reported
768 that ferroptosis makes OSA cells more susceptible to
769 doxorubicin, collaboratively strengthening the
770 apoptosis-based doxorubicin chemotherapy [43].
771 Therefore *A. annua* may be especially effective in
772 treating drug resistant osteosarcomas. Considering
773 the similarities between many human and canine
774 tumours, advances in deepening knowledge and
775 improving therapeutic protocols may be relevant for
776 both species, in a model of mutual translational
777 medicine. The relevance of *A. annua* as anticancer
778 compound is enhanced by the fact that it is cheap, as
779 compared to other pharmacological interventions
780 available on the market. This could be an advantage
781 for low-income countries [44] or contexts such as for
782 the dog owners' reluctance to choose chemotherapy
783 treatments.

4. Conclusions

The idroalcoholic extract of *A. annua* showed cytotoxicity on two canine OSA cell lines with increase of total iron, accumulation of lipid peroxides and a “ballooning” death phenotype, suggesting the activation of ferroptosis. However, it should be emphasized that any conclusions from this study must necessarily be confirmed on more cell lines.

Author Contributions:

Conceptualization: GI, GA, MF

Methodology: RS, CB, DLM, AZ, MF, GA, LM, MP

Validation, formal analysis: RS, CB, DLM, AZ, MF, GA, GI, LM, MP

Data curation: RS, CB, DLM, AZ, MF, GA, LM

Writing—original draft preparation: GI, RS, LM

Writing— review and editing: GI, GA, LM, MP

Project administration and funding acquisition: GI.

All authors have read and agreed to the published version of the manuscript.

F**unding**: This research was supported by a grant from “Fondazione Carisbo” (Bologna) (2019.0535, project title:

Attività antitumorale di estratti di *Artemisia* in colture cellulari di osteosarcoma di cane: un progetto multidisciplinare di medicina traslazionale).

Conflicts of Interest: The authors declare no conflict of interest.

References

1. Tu Y. The discovery of artemisinin (qinghaosu) and gifts from Chinese medicine. Nat Med. 2011;17:1217–20.

2. Efferth T. From ancient herb to modern drug: Artemisia annua and artemisinin for cancer therapy. Semin Cancer Biol. 2017;46:65–83.

3. Ho WE, Peh HY, Chan TK, Wong WSF. Artemisinins: pharmacological actions beyond anti-malarial. Pharmacol Ther. 2014;142:126–39.

4. Zhu S, Yu Q, Huo C, Li Y, He L, Ran B, et al. Ferroptosis: A Novel Mechanism of Artemisinin and its Derivatives in Cancer Therapy. Curr Med Chem. 2021;28:329–45.

5. Torti SV, Torti FM. Iron and cancer: more ore to be mined. Nat Rev Cancer. 2013;13:342–55.

6. Krishna S, Uhlemann A-C, Haynes RK. Artemisinins: mechanisms of action and potential for resistance. Drug Resist Updat. 2004;7:233–44.

7. Farcas N, Arzi B, Verstraete FJM. Oral and maxillofacial osteosarcoma in dogs: a review: Canine oral osteosarcoma. Vet Comp

Oncol. 2014;12:169–80.

8. Chen G-Q, Benthani FA, Wu J, Liang D, Bian Z-X, Jiang X. Artemisinin compounds sensitize cancer cells to ferroptosis by regulating iron homeostasis. Cell Death Differ. 2020;27:242–54.

9. Gola C, Giannuzzi D, Rinaldi A, Iussich S, Modesto P, Morello E, et al. Genomic and Transcriptomic Characterization of Canine Osteosarcoma Cell Lines: A Valuable Resource in Translational Medicine. Front Vet Sci. 2021;8:666838.

10. Massimini M, Romanucci M, De Maria R, Della Salda L. An Update on Molecular Pathways Regulating Vasculogenic Mimicry in Human Osteosarcoma and Their Role in Canine Oncology. Front Vet Sci. 2021;8:722432.

11. Sánchez-Céspedes R, Accornero P, Miretti S, Martignani E, Gattino F, Maniscalco L, et al. In vitro and in vivo effects of toceranib phosphate on canine osteosarcoma cell lines and xenograft orthotopic models. Veterinary and Comparative Oncology. 2020;18:117–27.

12. Morello E, Martano M, Buracco P. Biology, diagnosis and treatment of canine appendicular osteosarcoma: Similarities and differences with human osteosarcoma. The Veterinary Journal. 2011;189:268–77.

13. Meuten DJ, editor. Tumors in Domestic Animals. Hoboken, NJ, USA: John Wiley & Sons, Inc.; 2016.

14. Hosoya K, Murahari S, Laio A, London CA, Couto CG, Kisseberth WC. Biological activity of dihydroartemisinin in canine osteosarcoma cell lines. Am J Vet Res. 2008;69:519–26.

15. Isani G, Bertocchi M, Andreani G, Farruggia G, Cappadone C, Salaroli R, et al. Cytotoxic Effects of Artemisia annua L. and Pure Artemisinin on the D-17 Canine Osteosarcoma Cell Line. Oxid Med Cell Longev. 2019;2019:1615758.

16. Culurciello R, Bosso A, Di Fabio G, Zarrelli A, Arciello A, Carella F, et al. Cytotoxicity of an Innovative Pressurised Cyclic Solid-Liquid (PCSL) Extract from Artemisia annua. Toxins (Basel). 2021;13:886.

17. Protti M, Mandrioli R, Mandrone M, Cappadone C, Farruggia G, Chiocchio I, et al. Analysis of Artemisia annua extracts and related products by high performance liquid chromatography-tandem mass spectrometry coupled to sample treatment miniaturisation. J Pharm Biomed Anal. 2019;174:81–8.

18. Levi M, Salaroli R, Parenti F, De Maria R, Zannoni A, Bernardini C, et al. Doxorubicin treatment modulates chemoresistance and affects the cell cycle in two canine mammary tumour cell lines. BMC Vet Res. 2021;17:30.

19. Fox MH. A model for the computer analysis of synchronous DNA distributions obtained by flow cytometry. Cytometry. 1980;1:71–7.

20. Tüzen M. Determination of heavy metals in soil, mushroom and plant samples by atomic absorption spectrometry. Microchemical Journal. 2003;74:289–97.

21. Dixon SJ, Lemberg KM, Lamprecht MR, Skouta R, Zaitsev EM, Gleason CE, et al. Ferroptosis: an iron-dependent form of nonapoptotic cell death. Cell. 2012;149:1060–72.

22. Bai H, Wang C, Chen J, Peng J, Cao Q. A novel sensitive electrochemical sensor based on in-situ polymerized molecularly

880 imprinted membranes at graphene modified electrode for artemisinin
881 determination. Biosens Bioelectron. 2015;64:352–8.

882 23. Soktoeva TE, Ryzhova GL, Dychko KA, Khasanov VV,
883 Zhigzhitzhapova SV, Radnaeva LD. Artemisinin content in Artemisia
884 annua L. extracts obtained by different methods. Russ J Bioorg Chem.
885 2013;39:761–4.

886 24. Saeed MEM, Breuer E, Hegazy M-EF, Efferth T. Retrospective
887 study of small pet tumors treated with Artemisia annua and iron. Int J
888 Oncol. 2020;56:123–38.

889 25. Ferreira JFS, Luthria DL, Sasaki T, Heyerick A. Flavonoids from
890 Artemisia annua L. as antioxidants and their potential synergism with
891 artemisinin against malaria and cancer. Molecules. 2010;15:3135–70.

892 26. Efferth T, Herrmann F, Tahrani A, Wink M. Cytotoxic activity of
893 secondary metabolites derived from Artemisia annua L. towards
894 cancer cells in comparison to its designated active constituent
895 artemisinin. Phytomedicine. 2011;18:959–69.

896 27. Fenger JM, London CA, Kisseberth WC. Canine osteosarcoma: a
897 naturally occurring disease to inform pediatric oncology. ILAR J.
898 2014;55:69–85.

899 28. Ji Y, Zhang Y-C, Pei L-B, Shi L-L, Yan J-L, Ma X-H. Anti-tumor
900 effects of dihydroartemisinin on human osteosarcoma. Mol Cell
901 Biochem. 2011;351:99–108.

902 29. Greenshields AL, Fernando W, Hoskin DW. The anti-malarial
903 drug artesunate causes cell cycle arrest and apoptosis of triple-negative
904 MDA-MB-468 and HER2-enriched SK-BR-3 breast cancer cells. Exp
905 Mol Pathol. 2019;107:10–22.

30. Simpson S, Dunning MD, de Brot S, Grau-Roma L, Mongan NP, Rutland CS. Comparative review of human and canine osteosarcoma: morphology, epidemiology, prognosis, treatment and genetics. Acta Vet Scand. 2017;59:71.

31. Kuczler MD, Olseen AM, Pienta KJ, Amend SR. ROS-induced cell cycle arrest as a mechanism of resistance in polyaneuploid cancer cells (PACCs). Prog Biophys Mol Biol. 2021;165:3–7.

32. Matsui A, Hashiguchi K, Suzuki M, Zhang-Akiyama Q-M. Oxidation resistance 1 functions in the maintenance of cellular survival and genome stability in response to oxidative stress-independent DNA damage. Genes Environ. 2020;42:29.

33. Brown RAM, Richardson KL, Kabir TD, Trinder D, Ganss R, Leedman PJ. Altered Iron Metabolism and Impact in Cancer Biology, Metastasis, and Immunology. Front Oncol. 2020;10:476.

34. De Vico G, Martano M, Maiolino P, Carella F, Leonardi L. Expression of transferrin receptor-1 (TFR-1) in canine osteosarcomas. Vet Med Sci. 2020;6:272–6.

35. Cerchiaro G, Manieri TM, Bertuchi FR. Analytical methods for copper, zinc and iron quantification in mammalian cells. Metallomics. 2013;5:1336–45.

36. Lin H, Chen X, Zhang C, Yang T, Deng Z, Song Y, et al. EF24 induces ferroptosis in osteosarcoma cells through HMOX1. Biomedicine & Pharmacotherapy. 2021;136:111202.

37. Dodson M, Castro-Portuguez R, Zhang DD. NRF2 plays a critical role in mitigating lipid peroxidation and ferroptosis. Redox Biol. 2019;23:101107.

38. Valko M, Leibfritz D, Moncol J, Cronin MTD, Mazur M, Telser J. Free radicals and antioxidants in normal physiological functions and human disease. Int J Biochem Cell Biol. 2007;39:44–84.

39. Macotpet A, Suksawat F, Sukon P, Pimpakdee K, Pattarapanwichien E, Tangrassameeprasert R, et al. Oxidative stress in cancer-bearing dogs assessed by measuring serum malondialdehyde. BMC Vet Res. 2013;9:101.

40. Yan Z-Q, Wang D-D, Ding L, Cui H-Y, Jin H, Yang X-Y, et al. Mechanism of artemisinin phytotoxicity action: induction of reactive oxygen species and cell death in lettuce seedlings. Plant Physiol Biochem. 2015;88:53–9.

41. Kakhlon O, Cabantchik ZI. The labile iron pool: characterization, measurement, and participation in cellular processes(1). Free Radic Biol Med. 2002;33:1037–46.

42. Hattinger CM, Patrizio MP, Fantoni L, Casotti C, Riganti C, Serra M. Drug Resistance in Osteosarcoma: Emerging Biomarkers, Therapeutic Targets and Treatment Strategies. Cancers (Basel). 2021;13:2878.

43. Fu J, Li T, Yang Y, Jiang L, Wang W, Fu L, et al. Activatable nanomedicine for overcoming hypoxia-induced resistance to chemotherapy and inhibiting tumor growth by inducing collaborative apoptosis and ferroptosis in solid tumors. Biomaterials. 2021;268:120537.

44. Waseem Y, Hasan CA, Ahmed F. Artemisinin: A Promising Adjunct for Cancer Therapy. Cureus. 2018;10:e3628.